ChemPubSoc Europe

DOI: 10.1002/chem.201405733

CHEMISTRY A European Journal Communication

Natural Products

Divalent Transition-Metal-Ion Stress Induces Prodigiosin Biosynthesis in *Streptomyces coelicolor* M145: Formation of Coeligiosins

Anne Morgenstern,[b] Christian Paetz,[b] Anne Behrend,[b] and Dieter Spiteller*[a, b]

Abstract: The bacterium *Streptomyces coelicolor* M145 reacts to transition-metal-ion stress with myriad growth responses, leading to different phenotypes. In particular, in the presence of Co^{2+} ions (0.7 mM) *S. coelicolor* consistently produced a red phenotype. This phenotype, when compared to the wild type, differed strongly in its production of volatile compounds as well as high molecular weight secondary metabolites. LC-MS analysis revealed that in the red phenotype the production of the prodigiosins, undecylprodigiosin and streptorubin B, was strongly induced and, in addition, several intense signals appeared in the LC-MS chromatogram. Using LC-MS/MS and NMR spectroscopy, two new prodigiosin derivatives were identified, that is, coeligiosin A and B, which contained an additional undecylpyrrolyl side chain attached to the central carbon of the tripyrrole ring system of undecylprodigiosin or streptorubin B. This example demonstrates that environmental factors such as heavy metal ion stress can not only induce the production of otherwise not observed metabolites from so called sleeping genes but alter the products from well-studied biosynthetic pathways.

In their natural environment, microorganisms such as Actinomyces have to cope with changing and sometimes adverse conditions. Microorganisms not only rapidly adapt under evolutionary pressure[1] but their genomes contain a great repertoire of secondary metabolite genes[2] that can ensure their survival.

Actinomyces are most well-known for their secondary metabolites, such as polyketides or non-ribosomal peptides, many of which turned out to be of invaluable pharmaceutical use, for example, as antibiotics.[3]

[a] *Prof. Dr. D. Spiteller*
Chemical Ecology/Biological Chemistry
University of Konstanz
Universitätsstrasse 10
78457 Konstanz (Germany)
E-mail: dieter.spiteller@uni-konstanz.de

[b] *Dr. A. Morgenstern, Dr. C. Paetz, Dr. A. Behrend, Prof. Dr. D. Spiteller*
Max Planck Institute for Chemical Ecology
Hans Knöll Strasse 8
07745 Jena (Germany)

Supporting information for this article is available on the WWW under http://dx.doi.org/10.1002/chem.201405733.

The variation of fermentation conditions has been intensively used in order to optimize the production of secondary metabolites in biotechnological processes.[4] Bode et al. systematically varied growth conditions in order to induce the formation of diverse secondary metabolites in a selected Streptomyces strain and termed their approach OSMAC (one strain many compounds).[5] With the genome sequencing of many Actinomyces such as the model Streptomycete *Streptomyces coelicolor* A3(2),[6] it became evident that these antibiotic producers comprise a lot more secondary metabolite gene clusters than secondary metabolites that have been identified from them.[2,7]

Clearly, the maintenance of secondary metabolite gene clusters and their formation is costly for the producing strains.[8] In contrast to laboratory cultivation under optimized growth conditions, in their natural environment microorganisms have to cope with biotic and abiotic stress factors, for example, competition for space and nutrients. In such scenarios secondary metabolites are likely specifically and flexibly produced to ensure survival under varying and challenging growth conditions. In nature, therefore, microorganisms most likely produce secondary metabolites from "silent gene clusters" to react to their environment. Biotic and abiotic factors influence the microorganisms, leading to morphological and metabolic changes.[9–12]

The influence of such environmental factors can be studied in the laboratory, for example, by co-cultivation,[13,14] or by addition of antibiotics in subinhibitory concentrations,[10,15] signaling compounds,[9] or transition metal ions[16] such as Sc^{3+} ions[17,18] or Co^{2+} ions[19,20] into the growth medium.

Here, we studied the adaptation of *S. coelicolor* M145 (the source strain for the genome sequencing, not containing the plasmids SCP1 and SCP2 compared to *S. coelicolor* A3(2))[21] to suboptimal growth caused by transition metal ions that induced the formation of diverse phenotypes (Figure S1 in the Supporting Information), in particular a red phenotype (Figure S1 C in the Supporting Information) in *S. coelicolor* M145. Its secondary metabolite production strongly differed from the grey phenotype. The most obvious differences in its metabolic profile turned out to be due to changes in the prodigiosin biosynthesis of *S. coelicolor* M145,[22] yielding novel prodigiosin derivatives rather than the activation of silent secondary metabolite gene clusters.

In order to investigate how *S. coelicolor* M145 reacts to abiotic stress it was grown on soy flour medium (SFM) agar plates supplemented with different transition metal ions (Fe^{2+}, Mn^{2+}, Co^{2+}, Ni^{2+}, Cu^{2+}, Zn^{2+}, Cr^{2+}) in varying concen-

trations (0.1–30 mM). At certain concentrations, most of the metal ions used caused reduced growth and often hampered spore pigment formation (Figure S1 F in the Supporting Information).

With Co^{2+} ions (0.7 mM) we observed the formation of differently pigmented *S. coelicolor* M145 colonies that did not occur on control SFM agar plates. Interestingly, Co^{2+} ions led to myriad growth (Figure S1 A in the Supporting Information) in *S. coelicolor*: differently pigmented and shaped colonies occurred under Co^{2+}-ion stress (Figure S1 A,C,D,E in the Supporting Information), whereas without addition of Co^{2+}-ions *S. coelicolor* appeared on SFM medium as brown/grey colonies (Figure S1 B in the Supporting Information).

In the presence of Co^{2+}-ions (0.7 mM), red *S. coelicolor* colonies were regularly found on the SFM plates (Figure S1 C in the Supporting Information). These red colonies were picked and the phenotype could be maintained both on agar plates supplemented with Co^{2+}-ions and liquid medium supplemented with Co^{2+}-ions. Therefore, this red phenotype was selected in order to screen for differences in its secondary metabolite production compared to the untreated *S. coelicolor* grey phenotype.

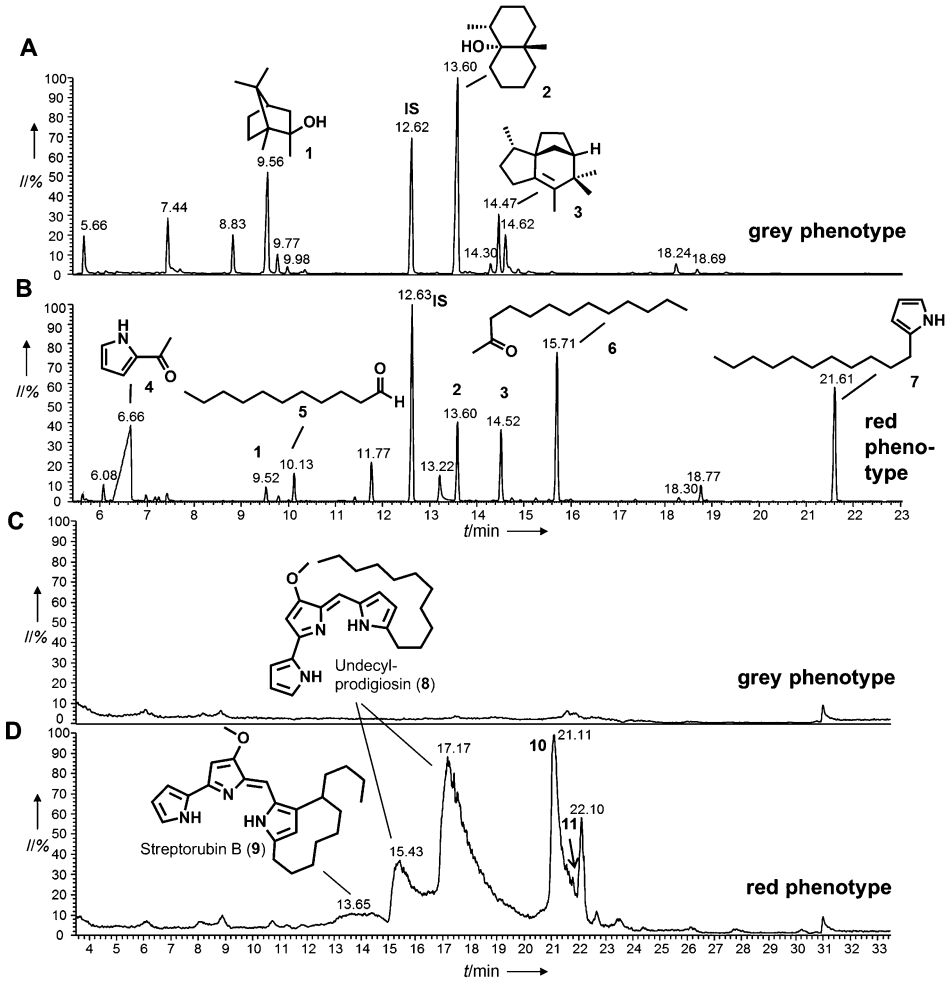

Figure 1. Metabolic differences of the *S. coelicolor* M145 grey phenotype and the red phenotype: GC-MS profiles of volatiles emitted by the grey phenotype (A) and the red phenotype (B) after 12 d (IS = internal standard). Comparison of the LC-ESI-MS chromatograms of methanolic cell extracts of the grey phenotype (C) and red phenotype (D) grown in SFM medium for 7 d.

First, we investigated the volatile profile of the red phenotype growing in SFM medium supplemented with Co^{2+}-ions for 3 to 12 d using SPME (solid phase micro extraction) and closed-loop stripping (CLS)[23] for volatile collection and GC-MS for their analysis (Figure 1).

Drastic changes in the volatile bouquet of the red phenotype were observed in comparison to the *S. coelicolor* M145 grey phenotype, which produced mainly 2-methylisoborneol (**1**) and geosmin (**2**) (Figure 1 A,B).[24] The red phenotype instead produced large amounts of 2-acetylpyrrole (**4**), 2-tridecanone (**6**), 2-undecylpyrrole (**7**), and only reduced amounts of 2-methylisoborneol (**1**) and geosmin (**2**) (see the Supporting Information). The intense peak of 2-undecylpyrrole (**7**) in the gas chromatogram of the volatiles from the red phenotype, together with its dark red pigmentation, suggested that in the red phenotype the production of the red colored prodigiosins, undecylprodigiosin (**8**) and streptorubin B (**9**) (Scheme 1),[25–28] might be strongly induced compared to the grey phenotype, when grown in SFM medium.

Both prodigiosins **8** and **9** are well-known secondary metabolites from *S. coelicolor* M145. They are biosynthesized by condensation of 4-methoxy-2,2′-bipyrrole-5-carboxaldehyde and 2-undecylpyrrole (**7**).[29] 2-Tridecanone (**6**) in the volatile profile of the red phenotype is likely a breakdown product of the 3-oxotridecanoylCoA ester, the biosynthetic precursor of 2-undecylpyrrole (**7**)[22] (see the Supporting Information).

The following differential analysis of methanolic cell extracts of the red phenotype and the grey phenotype by LC-MS revealed drastic differences in the production of secondary metabolites. The total ion current chromatogram of the red phenotype exhibited intense peaks corresponding to undecylprodigiosin at 15.4 min and 17.2 min (possibly different conformers)[27,28,30] (**8**) and streptorubin B (**9**) at 13.7 min, and additional peaks of so far unknown compounds that were not produced by the grey phenotype (Figure 1 C/D). The prodigiosins, undecylprodigiosin (**8**) and streptorubin B (**9**), were purified and

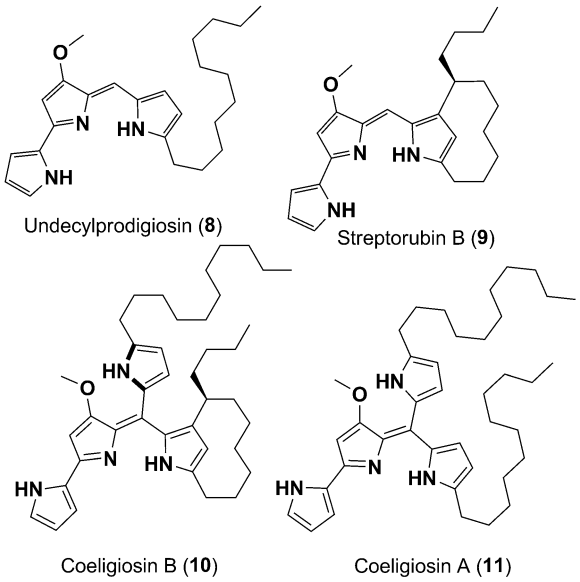

Scheme 1. Structures of undecylprodigiosin (**8**), streptorubin B (**9**), and the novel prodigiosin derivatives coeligiosin B (**10**) and coeligiosin A (**11**).

confirmed by HR-ESI-MS and NMR. One of the unknown compounds (**10**) was isolated using size exclusion chromatography, flash chromatography, solid phase extraction, and semipreparative HPLC. **10** was obtained as a dark purple solid (ca. 0.1 mg L^{-1} culture) with a $[M+H]^+$ ion of $m/z = 611.46857$ corresponding to the molecular formula $C_{40}H_{58}ON_4$. The compound contained 14 double bond equivalents, suggesting the presence of an extended aromatic system in the molecule. Because the quasimolecular ion of **10** fragmented in a similar way as the quasimolecular ion of streptorubin B (**9**),[31] it is clear that both compounds were closely related (see the Supporting Information). Consequently, we subtracted the elemental composition of streptorubin B (**9**) from the unknown compound **10**. The difference was $C_{15}H_{25}N$, matching to an additional 2-undecylpyrrolyl moiety. Thus, the structure of **10** could be a streptorubin B (**9**) derivative with an additional 2-undecylpyrrolyl side chain (Figure 2 A).

NMR analysis of **10** in CD_3OD at 298 K (Figure 2 B) revealed instantly significant similarities to undecylprodigiosin (**8**) and streptorubin B (**9**). Six proton signals at $\delta = 6.2$–7.1 ppm corresponding to seven pyrrole protons and an intense signal for alkyl protons ($\delta = 0.76$–1.47 ppm) were observed, with the latter matching two undecyl side chains.

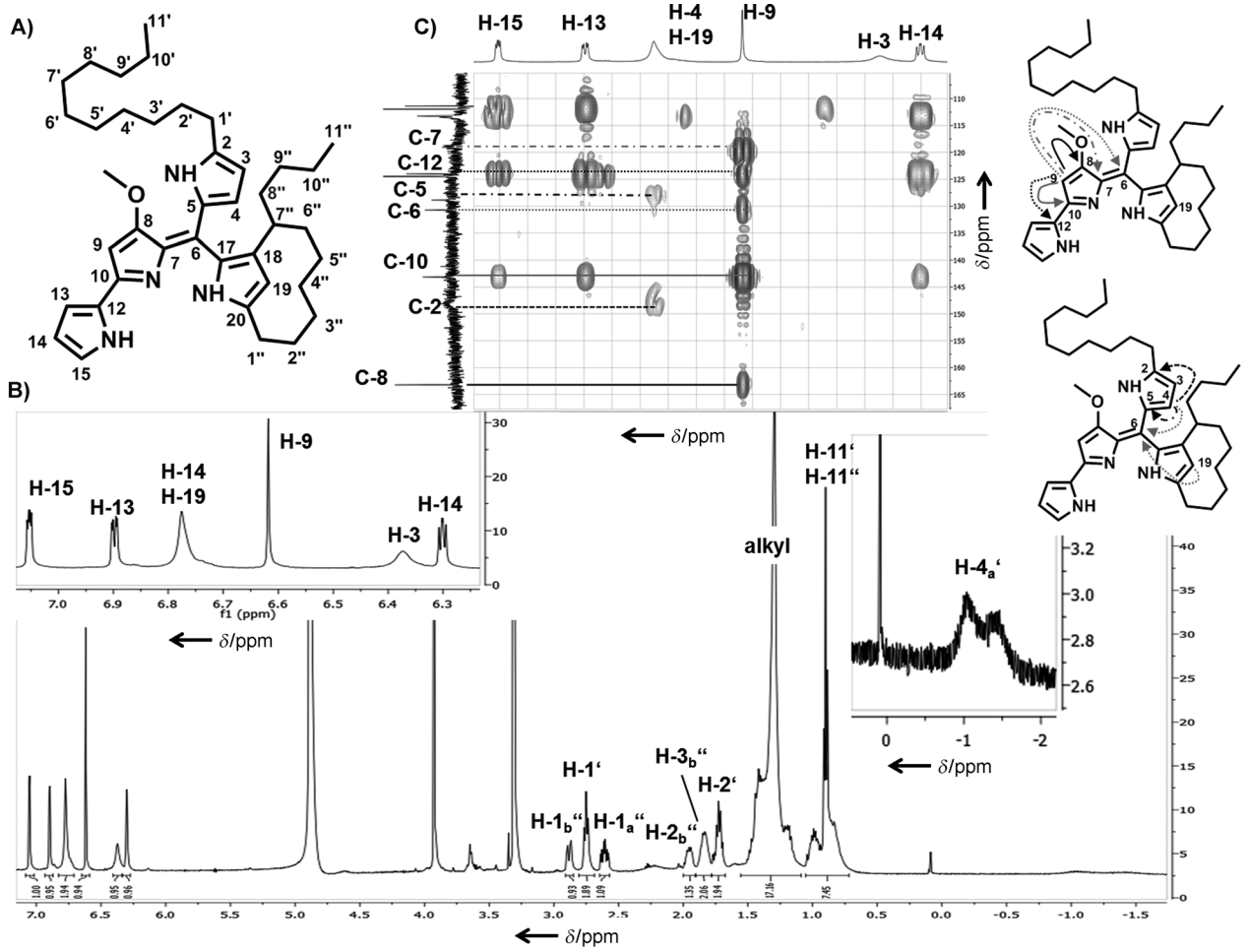

Figure 2. Structure elucidation of **10**: A) Structure of coeligiosin B (**10**); B) ^{1}H NMR spectrum of **10**; C) selected aromatic region of the HMBC spectrum of **10**.

However, in comparison to the NMR spectra of prodigiosins **8** and **9** the line shapes of the aromatic protons of **10** were rather broad, particularly the signals for H-3, H-4, and H-19. Other solvents such as $CDCl_3$, C_6D_6 CD_3CN, and $[D_6]$DMSO did not result in better spectra compared to those in CD_3OD at 298 K, but revealed the presence of three exchangeable NH protons. The extended conjugated system of **10** with the additional pyrrole moiety in comparison to the prodigiosins **8** and **9** clearly causes the observed line broadening.

The ^{1}H-^{1}H-COSY correlations of **10** accounted for one pyrrole moiety substituted at position 2, two pyrrole rings substituted at three carbon atoms, and one pyrrole moiety substituted at the positions 2 and 5. In the ^{1}H NMR spectrum of **10** the proton signal of the central carbon atom C-6, like that found in the spectrum of undecylprodigiosin (**8**) or streptorubin B (**9**), was missing, suggesting that the additional 2-undecylpyrrolyl moiety of **10** is attached at this position. The attachment of the 2-undecylpyrrolyl moiety to the streptorubin B core structure at the central carbon C-6 was also reflected in ^{1}H-^{13}C-HMBC correlations of H-4, H-19, and H-9 to C-6 (Figure 2C). However, the cross signal of H-4 and H-19 to C-6 was very weak (likely due to dynamic effects) and was only obtained by using ^{1}H-^{13}C-HMBC conditions favoring the detection of ^4J signals (CNST13 = 5 Hz). The carbon atom C-6 was assigned to be quaternary at δ_c130.7 according to the absence of a ^{1}H-^{13}C-HSQC correlation, which fits with the assumption that C-6 of **10** is being substituted with the additional 2-undecylpyrrolyl moiety.

In order to elucidate the carbocyclic ring in **10** we searched for the H-4″ signal for which the corresponding signal in streptorubin B (**9**) appears at δ_H −1.44.[27] The H-4$_a$″ signal of **10** appeared at δ_H −0.83−−1.64, but it was very broad and thus hardly visible (Figure 2B).

Because of the shortcomings of the NMR spectra of **10** in CD_3OD at 298 K, the behavior of **10** at different temperatures was studied. Cooling to 222 K led to significant changes in the signal pattern (see the Supporting Information). The broad signals of H-4, H19, and H-3 changed to a set of signals indicating the presence of three conformers (major, minor, and trace isomer) of **10**. Instead of the hardly visible signal of H-4$_a$″ at 298 K, two well detectable signals at δ_H −0.95−−1.06 and δ_H −1.52−−1.63 appeared for H-4$_a$″ at 222 K. Although the mixture of conformers of **10** at 222 K complicated the NMR spectra, key ^{1}H-^{13}C-HMBC correlations to the central atom C-6 appeared clearer than at 298 K (see the Supporting Information). Based on the accumulated spectroscopic data we concluded that the novel compound **10** is a streptorubin B derivative with an additional 2-undecylpyrrolyl moiety attached to the central carbon atom (C-6) of the tripyrrole ring system of prodigiosins (Scheme 1). As with streptorubin B (**9**), **10** was expected to contain a 10-membered *meta*-bridged butylcycloheptylpyrrole moiety. However, due to overlapping signals, the connection of the carbocyclic ring was not identified by NMR but by feeding [1′,1′,7′,7′-$^2H_4$]-2-undecylpyrrole (**7′**) to the red phenotype and studying the incorporation of the deuterium atoms into **10** by LC-ESI-MS. [1′,1′,7′,7′-$^2H_4$]-2-undecylpyrrole (**7′**) was obtained from [7′,7′-$^2H_2$]-2-undecanoylpyrrole by sodium borodeuteride reduction. [7′,7′-$^2H_2$]-2-undecanoylpyrrole was synthesized by acylation of pyrrole magnesium chloride[22] with [7,7-$^2H_2$]-undecanoic acid, followed by ester hydrolysis (see the Supporting Information). LC-ESI-MS analysis of **10** after feeding [1′,1′,7′,7′-$^2H_4$]-2-undecylpyrrole to the red phenotype revealed increased isotope peaks at *m/z* 614 ($[M+3+H]^+$, cyclic side chain labeled), *m/z* 615 ($[M+4+H]^+$, linear side chain labeled), and 618 ($[M+7+H]^+$, both side chains labeled) (see the Supporting Information). The observed incorporation pattern into **10** proves that it consists of an analogous ten-membered carbocylic ring as streptorubin B (**9**), because one deuterium atom was lost upon ring formation with [1′,1′,7′,7′-$^2H_4$]-2-undecylpyrrole (**7′**, see the Supporting Information). The chiral carbon C-7″ of the carbocyclic chain in coeligiosin B (**10**) was assigned with *S*-configuration, as with that of streptorubin B (**9**),[27,28] based on the similar circular dichroism spectrum and the origin of the compound. At 298 K coeligiosin B (**10**) shows interconversion of its possible atropisomers, whereas at 222 K three conformers were observed. Roesy measurements suggest that the 2-undecylpyrrolyl moiety of the major isomer of **10** stands out of the plane formed by the streptomycin B core because of a clear correlation between C4 with C4″ (see the Supporting Information).

Because of its close relationship to streptorubin B (**9**) and its occurrence in *S. coelicolor*, we named compound **10** coeligiosin B (Scheme 1).

Besides coeligiosin B (**10**), a closely related compound (**11**) with a quasimolecular ion of *m/z* 613.48407, corresponding to an elemental composition of $C_{40}H_{60}ON_4$, was found by LC-MS analysis of the methanolic extract of the red phenotype.

Compound **11** differed from coeligiosin B (**10**) by two additional hydrogen atoms. In analogy to the prodigiosins, streptorubin B (**9**) and undecylprodigiosin (**8**), which also differ by two hydrogens due to the carbocylic ring of the undecyl side chain, **11** was suspected to be an undecylprodigiosin (**8**) with an additional undecylpyrrolyl side chain and consequently we named it coeligiosin A (**11**). The comparison of the MS/MS spectrum of coeligiosin A (**11**) with coeligiosin B (**10**), undecylprodigiosin (**8**), and streptorubin B (**9**) fully supported this assignment (see the Supporting Information). The quasimolecular ion of coeligiosin A (**11**) fragments to a series of ions that reflect the 2 amu difference to coeligiosin B (**3**) (see the Supporting Information). However, compound **11** was produced in such low amounts by the red phenotype that our deductions based on mass spectrometry could not be supported by additional NMR spectra.

To rule out that coeligiosins might be formed during the work-up, we analyzed colonies of the red phenotype directly from SFM agar plates by MALDI-MS. Prodigiosins and coeligiosins were found and it became evident that coeligiosins were produced by the red phenotype. Because the MALDI-MS detection worked very well, we also applied it to screen red colonies of *S. coelicolor* M145 grown in the presence of different transition metal ions (Fe^{2+}, Mn^{2+}, Co^{2+}, Ni^{2+}, Cu^{2+}, and Zn^{2+}). Most transition metal ions apart from Fe^{2+} induced the formation of prodigiosins and coeligiosins (see the Supporting Information). The induction of the prodigiosin biosynthesis and its alteration

to additionally produce coeligiosins is not restricted to Co^{2+} ions but occurs with several transition-metal ions.

So far, the biosynthesis of coeligiosins still remains unclear; besides that, there is a clear overproduction of the precursor 2-undecylpyrrole (**7**). For the additional attachment of 2-undecylpyrrole (**7**), an oxidation of the central carbon C-6 of streptorubin B (**9**) or of the aldehyde moiety of 4-methoxy-2,2′-bipyrrole-5-carboxaldehyde is expected.

In addition to future biosynthetic studies, the molecular basis for the observed phenotype also needs further investigation. At the moment we cannot tell if the red phenotype was caused by a transition-metal-induced mutation or by a regulatory effect. If the red phenotype is propagated on medium without the addition of Co^{2+} ions the red phenotype is gradually lost and the appearance of the resulting strain becomes similar to the grey phenotype, which might be due to back mutation or cancellation of a regulatory effect.

In summary, transition-metal-ion stress caused the formation of diverse *S. coelicolor* M145 phenotypes. The red phenotype showed a drastically altered secondary metabolite profile. The production of undecylprodigiosin (**8**) and streptorubin B (**9**) was strongly induced. In addition, we detected the formation of the so far unknown prodigiosin derivatives, coeligiosins A (**11**) and B (**10**).

Our observations show that environmental stress can cause metabolic flexibility of a well-known biosynthetic pathway in Streptomyces. Besides the induction of "silent gene clusters",[9,11,12] one has to consider other metabolic changes that may yield novel metabolites. Future experiments are needed to understand the adaptation of the prodigiosin biosynthesis,[22] as well as the molecular basis that led to the development of the red phenotype of *S. coelicolor* M145 under transition-metal-ion stress.

Experimental Section

General: Chemicals were purchased from Sigma Aldrich. Reactions were performed with dry solvents under argon atmosphere if necessary. GC-MS was performed with a Thermofisher TraceMS. For LC-MS a Dionex 3000 HPLC system connected to a Thermofisher LTQ fitted with an ESI ion source was used. AP-MALDI-MS was performed with the ion source from MassTech connected to the LTQ. HR-ESI-MS spectra were obtained from a Thermofisher Orbitrap XL. For semipreparative HPLC an Agilent 1100 HPLC system connected to a Gilson 206 fraction collector was used. NMR spectra were recorded with Bruker Avance AV-400, AV-600 or AV-500 spectrometer (the latter fitted with a TCI cryoprobe). NMR spectra were calibrated using the solvent signals (^{1}H NMR δ_H in ppm: $CDCl_3$ 7.26, CD_3OD 3.31, ^{13}C NMR δ_c in ppm: $CDCl_3$ 77.7, CD_3OD 49.00).

Strain and cultivation conditions: *S. coelicolor* M145 was grown on SFM agar plates (20 g soybean flour, 20 g mannitol, 15 g agar, 1 L ddH_2O)[21] at 28 °C. *S. coelicolor* M145 was challenged by addition of transition metal ions ($CoSO_4$, $CoCl_2$, $CuSO_4$, $CrCl_2$, $FeSO_4$, $ZnCl_2$, $NiSO_4$, $MnSO_4$,) to the agar plates in varying concentrations (0.1–30 mM). Because growth of *S. coelicolor* in presence of $CoSO_4$ (0.7 mM) reliably induced the formation of a red phenotype, it was used for further studies. For formation of the red phenotype, SFM agar plates (diameter 9 cm, 50 mL) were covered with 500 μL $CoSO_4$ solution (0.07 M). After drying of the $CoSO_4$ solution, *S. coelicolor* M145 spores were spread onto the agar plates. After about 5 d of incubation, different phenotypes were picked and cultivated on fresh SFM agar plates, containing $CoSO_4$ (0.7 mM).

For the comparison of the metabolic profiles of the grey phenotype and the red phenotype, cultures were supplemented with 0.7 mM $CoSO_4$ and cultivated in 200 mL of liquid SFM medium in 500 mL flasks fitted with springs for aeration. A single colony from SFM agar plates served as inoculum. The flasks were incubated on an Infors orbital shaker at 220 rpm at 28 °C for 10 d. 1 mL samples were withdrawn each day for 10 d. The samples were centrifuged (16000 g, 1 min). The pellet was resuspended in MeOH and extracted for 1 h. After centrifugation (16000 g, 2 min) the extract (5 μL) was analyzed by LC-MS.

LC-MS analysis: Methanolic cell extracts of *S. coelicolor* grey phenotype and the red phenotype were analyzed by LC-MS. The extracts were separated using a Gemini C18 (250 mm × 2 mm, 5 μm, Phenomenex) column. HPLC-conditions: A: H_2O 0.1% formic acid, B: MeCN 0.1% formic acid; HPLC programme: 2 min 30% B, 16 min to 70% B, 2 min to 100% B, 8 min 100% B; flow rate: 0.35 mL min^{-1}, injection volume: 1–50 μL.

Isolation of coeligiosins: 1 L *S. coelicolor* red phenotype was grown in SFM medium supplemented with $CoSO_4$ (0.7 mM) for 7 d (see above). The cells were harvested and extracted with 3× 250 mL acidified methanol overnight. After centrifugation (4000 g, 30 min), the supernatant was diluted with water (300 mL) and extracted with chloroform (3×200 mL), the organic layer was dried over Na_2SO_4 and evaporated to dryness. The residue was dissolved in methanol (15 mL) and applied to a Sephadex LH20 column (5× 50 cm). The compounds were eluted with methanol. Fractions containing coeligiosins from the LH20 size-exclusion chromatography were combined, concentrated, and separated using an XTerra MS C18 column (10 mm×50 mm, 5 μm, Waters). HPLC programme: 2 min 65% B, in 18 min to 100% B, 15 min 100% B; flow of 2 mL min^{-1}; solvent A: H_2O 0.5 AcOH, solvent B: MeOH 0.5 AcOH. Final purification was performed by silica flash column chromatography using chloroform/methanol/28% aqueous ammonia solution (95/5/1) as eluent.

Acknowledgements

D.S. thanks Prof. Dr. Boland for his generous support and the Deutsche Forschungsgemeinschaft for an Emmy Noether Fellowship (SP 1106/3-1). We are grateful to Anke Friemel for the NMR measurements at different temperatures.

Keywords: abiotic stress · antibiotics · induction · metabolism · natural products

[1] S. F. Elena, R. E. Lenski, *Nat. Rev. Genet.* **2003**, *4*, 457–469.
[2] M. Nett, H. Ikeda, B. S. Moore, *Nat. Prod. Rep.* **2009**, *26*, 1362–1384.
[3] A. L. Demain, *J. Ind. Microbiol. Biotechnol.* **2014**, *41*, 185–201.
[4] S. Parekh, V. A. Vinci, R. J. Strobel, *Appl. Microbiol. Biotechnol.* **2000**, *54*, 287–301.
[5] H. B. Bode, B. Bethe, R. Hofs, A. Zeeck, *ChemBioChem* **2002**, *3*, 619–627.
[6] S. D. Bentley, K. F. Chater, A. M. Cerdeno-Tarraga, G. L. Challis, N. R. Thomson, K. D. James, D. E. Harris, M. A. Quail, H. Kieser, D. Harper, A. Bateman, S. Brown, G. Chandra, C. W. Chen, M. Collins, A. Cronin, A. Fraser, A. Goble, J. Hidalgo, T. Hornsby, S. Howarth, C. H. Huang, T. Kieser, L. Larke, L. Murphy, K. Oliver, S. O'Neil, E. Rabbinowitsch, M. A.

Rajandream, K. Rutherford, S. Rutter, K. Seeger, D. Saunders, S. Sharp, R. Squares, S. Squares, K. Taylor, T. Warren, A. Wietzorrek, J. Woodward, B. G. Barrell, J. Parkhill, D. A. Hopwood, *Nature* **2002**, *417*, 141 – 147.
[7] G. L. Challis, *J. Ind. Microbiol. Biotechnol.* **2014**, *41*, 219 – 232.
[8] H. Jenke-Kodama, E. Dittmann, *Phytochemistry* **2009**, *70*, 1858 – 1866.
[9] V. Yoon, J. R. Nodwell, *J. Ind. Microbiol. Biotechnol.* **2014**, *41*, 415 – 424.
[10] P. Vaz Jauri, M. G. Bakker, C. E. Salomon, L. L. Kinkel, *PLoS One* **2013**, 81064.
[11] H. Zhu, S. K. Sandiford, G. P. van Wezel, *J. Ind. Microbiol. Biotechnol.* **2014**, *41*, 371 – 386.
[12] C. Hertweck, *Nat. Chem. Biol.* **2009**, *5*, 450 – 452.
[13] V. Schroeckh, K. Scherlach, H.-W. Nuetzmann, E. Shelest, W. Schmidt-Heck, J. Schuemann, K. Martin, C. Hertweck, A. A. Brakhage, *Proc. Natl. Acad. Sci. USA* **2009**, *106*, 14558 – 14563.
[14] M. F. Traxler, J. D. Watrous, T. Alexandrov, P. C. Dorrestein, R. Kolter, *mBio* **2013**, *4*, e00459-13.
[15] D. Romero, M. F. Traxler, D. Lopez, R. Kolter, *Chem. Rev.* **2011**, *111*, 5492 – 5505.
[16] G. Haferburg, I. Groth, U. Moellmann, E. Kothe, I. Sattler, *Biometals* **2009**, *22*, 225 – 234.
[17] K. Kawai, G. Wang, S. Okamoto, K. Ochi, *FEMS Microbiol. Lett.* **2007**, *274*, 311 – 315.
[18] Y. Tanaka, T. Hosaka, K. Ochi, *J. Antibiot.* **2010**, *63*, 477 – 481.
[19] U. Gräfe, I. Eritt, D. Riesenberg, *J. Basic Microbiol.* **1985**, *25*, 279 – 283.
[20] C. A. Claridge, V. Z. Rossoman, N. S. Buono, A. Gourevitch, J. Lein, *Appl. Microbiol.* **1966**, *14*, 280 – 283.
[21] S. Mo, P. K. Sydor, C. Corre, M. M. Alhamadsheh, A. E. Stanley, S. W. Haynes, L. Song, K. A. Reynolds, G. L. Challis, *Chem. Biol.* **2008**, *15*, 137 – 148.
[22] K. Grob, F. Zürcher, *J. Chromatogr.* **1976**, *117*, 285 – 294.
[23] S. Schulz, J. S. Dickschat, *Nat. Prod. Rep.* **2007**, *24*, 814 – 842.
[24] X. Lin, R. Hopson, D. E. Cane, *J. Am. Chem. Soc.* **2006**, *128*, 6022 – 6023.
[25] S. W. Tsao, B. A. M. Rudd, X. G. He, C. J. Chang, H. G. Floss, *J. Antibiot.* **1985**, *38*, 128 – 131.
[26] H. Laatsch, M. Kellner, H. Weyland, *J. Antibiot.* **1991**, *44*, 187 – 191.
[27] S. W. Haynes, P. K. Sydor, C. Corre, L. Song, G. L. Challis, *J. Am. Chem. Soc.* **2011**, *133*, 1793 – 1798.
[28] D. X. Hu, M. D. Clift, K. E. Lazarski, R. J. Thomson, *J. Am. Chem. Soc.* **2011**, *133*, 1799 – 1804.
[29] A. M. Cerdeño, M. J. Bibb, G. L. Challis, *Chem. Biol.* **2001**, *8*, 817 – 829.
[30] K. Chen, N. S. Rannulu, Y. Cai, P. Lane, A. L. Liebl, B. B. Rees, C. Corre, G. L. Challis, R. B. Cole, *J. Am. Soc. Mass Spectrom.* **2008**, *19*, 1856 – 1866.
[31] T. Kieser, M. J. Bibb, M. J. Buttner, K. F. Chater, D. A. Hopwood, *Practical Streptomyces Genetics*, John Innes Centre, Norwich, **2000**.

Received: October 20, 2014
Published online on March 11, 2015